



Full Length Article

Color converters for white LEDs using liquid phase epitaxy growth method

A. Markovskiy^{a,b,*}, V. Gorbenko^a, T. Zorenko^a, A. Fedorov^c, Yu Zorenko^{a,**}^a Faculty of Physics, Kazimierz Wielki University in Bydgoszcz, Powstańców Wielkopolskich Str., 2, 85090, Bydgoszcz, Poland^b Mechantronic Department, Kazimierz Wielki University in Bydgoszcz, Kopernik, 1, 85-074, Bydgoszcz, Poland^c Institute for Single Crystals, National Academy of Sciences of Ukraine, Av. Nauki 60, 61178, Kharkiv, Ukraine

ARTICLE INFO

Keywords:

Single crystalline films

Liquid phase epitaxy

Garnets

Ce³⁺ ions

Photoconverter

Planar-chip-level conversion

White LEDs

ABSTRACT

The development of innovative high-power lighting sources is urgently required to design and investigate the new high structural quality and high-temperature stable converters in the form of single crystals and single crystalline films. This research deals with the growth and investigation of structural, luminescence, and photoconversion properties (color coordinates, color temperature and color rendering index) of the single crystalline films of Ce³⁺ doped (Lu, Y, Tb, Gd)₃Al₅O₁₂ garnets, grown using the Liquid Phase Epitaxy method onto undoped Y₃Al₅O₁₂ substrates. The combination of Ce³⁺ doped Lu₃Al₅O₁₂, Y₃Al₅O₁₂, Tb₃Al₅O₁₂, Gd_{2.9}Lu_{0.1}Al₅O₁₂ film converter with respective thickness with commercial blue LED allows for obtaining green-yellow-orange-emitting pc-WLEDs. The application of the mentioned film converters results in the formation of four basic trends on the color diagram depending on the thickness of the converter.

1. Introduction

Recently garnets, oxynitrides, silicates, and aluminates have been actively studied as host materials for converting luminescence ions. However, the main research is focused on the garnet type lattices, such as Ce³⁺ doped Y₃Al₅O₁₂ (YAG:Ce) garnet, and nowadays, typical WLEDs consist of YAG:Ce phosphor powders encapsulated in epoxy resins on top of a blue LED. The function of the phosphor converter is to absorb the blue light emitted by the LED chip and convert it to yellow light, due to the Ce³⁺ ions luminescence. The combination of the transmitted blue light and yellow Ce³⁺ emission band due to the 5d-4f transitions allows for obtaining white light. The high flexibility of the {Ln}₃{M}₂(M)₃O₁₂ (Ln = Lu, Y, Gd, Tb; M = Al, Ga, Sc) garnet structure allows for replacing ions in dodecahedral {a}, octahedral [b] and tetrahedral (c) sites, and thus, to modify the composition for optimization of the Ce³⁺ luminescence properties demanded in WLED application. The influence of such composition engineering strategy is based on the “Ce³⁺ 5d level positioning” [1] and “band-gap engineering” [2]. The choice of cations allows for tuning of the local coordination environment of the luminescent ions and changes the crystal field strength and the covalence of Ce³⁺-O²⁻ bonding. Such changes in garnet composition allow for variation in the Ce³⁺ emission color from the green to the orange-red spectral range. The shift of YAG:Ce spectrum into the red range often is carried out by (i)

partial or full cationic substitution of Y³⁺ ions by larger Tb³⁺ or Gd³⁺ ions (composition engineering strategy); (ii) or codoping of YAG:Ce with red-emitting rare-earth ions (Eu³⁺, Mn²⁺) (codoping level control tuning) [3]. Such spectral tuning increases the luminescence efficiency of phosphor converted (pc)-WLEDs, optimizes the color conversion, achieves the desired color temperature, and increases the color gamut [4,5]. The widespread garnet solid solution variations enable tuning and optimization of optical, luminescence, and photoconversion properties depending on the area of application.

The temperature-quenching behavior of cerium-doped garnet-type phosphors holds significant relevance in practical applications, particularly within white LEDs (w-WLEDs). This importance is underscored by the fact that when phosphors are directly applied to blue-emitting (InGa)N chips, temperatures can exceed 100 °C and even approach 200 °C [6]. Thus, the quenching temperature of Ce³⁺ luminescence in garnets is an important parameter in the optimization of PC. An onset of Ce³⁺ luminescence quenching above 600 K for YAG:Ce and 700 K for LuAG:Ce was reported previously [7]. The quenching temperature is lowest for Ce³⁺ in Gd₃Al₅O₁₂ (GdAG), around 300 K, where the energy difference between the 5d₁ state and the conduction band edge is smallest [8].

The optical properties of phosphor-converters for white LEDs depend not only on the composition but also on the synthesis process, which

* Corresponding author. Faculty of Physics, Kazimierz Wielki University in Bydgoszcz, Powstańców Wielkopolskich str., 2, 85090, Bydgoszcz, Poland.

** Corresponding author.

E-mail addresses: a.mark@ukw.edu.pl (A. Markovskiy), zorenko@ukw.edu.pl (Y. Zorenko).

largely determines the type of impurities, homogeneity, induced defects, microstructure, morphology, etc. in the most powerful LEDs. For the development of innovative high-power lighting sources, it is urgently needed to design and investigate the new high structural quality and high-temperature stable converters in the form of single crystals and single crystalline films (SCF) [9]. The liquid phase epitaxy (LPE) technique is a versatile method for the production of SCFs for applications in optoelectronics with thicknesses in the range of several micrometers up to 200 μm with excellent material quality and reproducibility [10].

In the quasi-homoepitaxy LPE process, the materials of the same class are grown, and only one component is substituted by another. However, such substitutions of the first material do not lead to a fundamental change in its physical properties since it belongs to the same chemical group as the second material, for example, the $\text{Lu}_3\text{Al}_5\text{O}_{12}:\text{Ce}$ (LuAG:Ce) and $\text{Tb}_3\text{Al}_5\text{O}_{12}:\text{Ce}$ (TbAG:Ce) SCFs grown on YAG substrates. The main limitations for the quasi-homoepitaxy growth of garnets are associated with the selection of a single-crystal substrate on which the film will be grown. For this technique, the permissible lattice constant misfit between the film and the substrate is considered to be in the range $\Delta m = (a_{\text{SCF}} - a_{\text{sub}})/a_{\text{sub}} \times 100 = \pm 1.0\%$ [11–13]. The YAG is a relatively cheap substrate commonly used in LPE for the growth of high-quality single crystalline films [11–13]. YAG's crystal lattice parameter 12.008 \AA closely matches that of all garnet family members, from LuAG (11.91 \AA) to GdAG (12.113 \AA) [11,12,14], enabling defect-free film growth with a high degree of crystallographic orientation.

The stability of the garnet crystal structure relies on the size of trivalent lanthanide ions (Ln^{3+}). It's stable for smaller ions (Tb^{3+} , Lu^{3+} , Y^{3+}) and not for larger ones Gd^{3+} acting as the cutoff. Adding smaller Lu^{3+} ions to GdAG, and creating (Gd, Lu)AG solid solutions enhances the stability of the garnet structure. In particular, information about the luminescence properties of Ce^{3+} -doped gadolinium aluminum garnet GdAG is limited by few studies [15,16]. The lattice parameters of (Gd, Lu)AG can be close to YAG when doped with 45 at.% Lu^{3+} [12]. In addition, GdAG-based transparent ceramics are often doped with Ga^{3+} to stabilize the lattice [17].

One of the first works in the area of SCF converters for WLEDs was done by Kundaliya et al. [18] and recently by our group [19], who proposed phosphor-converter production by depositing a YAG:Ce and LuAG:Ce garnet phosphor film epitaxially onto a YAG substrate, to induce yellow and green emission, respectively. In this work, comprehensive studies have been carried out to investigate various LPE grown film photoconverters with different compositions and thicknesses in the allowable region of SCF crystallization of $\{\text{Lu}, \text{Y}, \text{Tb}, \text{Gd}\}_3\text{Al}_5\text{O}_{12}$ garnets onto YAG substrates.

2. Sample preparation and experimental methods

The six groups of Ce^{3+} doped $\{\text{Lu}, \text{Y}, \text{Tb}, \text{Gd}\}_3\text{Al}_5\text{O}_{12}$ garnets, listed in Table 1, were grown using the LPE method onto undoped $\text{Y}_3\text{Al}_5\text{O}_{12}$ (YAG) substrates with (110) orientation (Fig. 1). LPE growth was performed in the LPE lab at the Chair for Optoelectronic Materials of the Department of Physics of Kazimierz Wielki University in Bydgoszcz, Poland onto YAG substrates, prepared from single crystals (SC) grown by the Czochralski method in Crytur Ltd. Czech Republic. The SCF samples with demanded compositions were grown by the LPE method from the supercooled melt solution based on $\text{PbO}-\text{B}_2\text{O}_3$ (12:1 mol/mole) flux and 4 N purity garnet-forming oxides: Lu_2O_3 , Y_2O_3 , Tb_4O_7 , Gd_2O_3 , Al_2O_3 and CeO_2 , placed in Pt crucible.

The Blank-Nielsen coefficients R_1 , R_2 , R_3 , and R_4 (Eq. 1) should be maintained during the preparation of the melt solution for the production of SCF with chosen content, and they should correspond to the following molar ratios [13]:

Table 1

The nominal composition of garnet SCFs under study and Ce^{3+} concentration range related to the formula unit (h is the SCFs thickness).

Nominal composition	Actual composition	h, μm	CeO_2 content in the melt solution, mole %	Ce content in the SCF, at. %
$\text{Lu}_3\text{Al}_5\text{O}_{12}:\text{Ce}$		78, 92, 162	12	0.075
$\text{Lu}_2\text{TbAl}_5\text{O}_{12}:\text{Ce}$	$\text{Lu}_{1.85}\text{Tb}_{1.15}\text{Al}_5\text{O}_{12}:\text{Ce}$	22, 27, 36	10	0.1
$\text{Y}_3\text{Al}_5\text{O}_{12}:\text{Ce}$		30, 41, 46	10	0.1
$\text{Tb}_3\text{Al}_5\text{O}_{12}:\text{Ce}$		30, 36, 44	8	0.15
$\text{Tb}_{1.5}\text{Gd}_{1.5}\text{Al}_5\text{O}_{12}:\text{Ce}$	$\text{Tb}_{1.62}\text{Gd}_{1.38}\text{Al}_5\text{O}_{12}:\text{Ce}$	45, 55, 76	8	0.15
$\text{Gd}_{2.9}\text{Lu}_{0.1}\text{Al}_5\text{O}_{12}:\text{Ce}$	$\text{Gd}_{2.84}\text{Lu}_{0.16}\text{Al}_5\text{O}_{12}:\text{Ce}$	74, 86	10	0.15

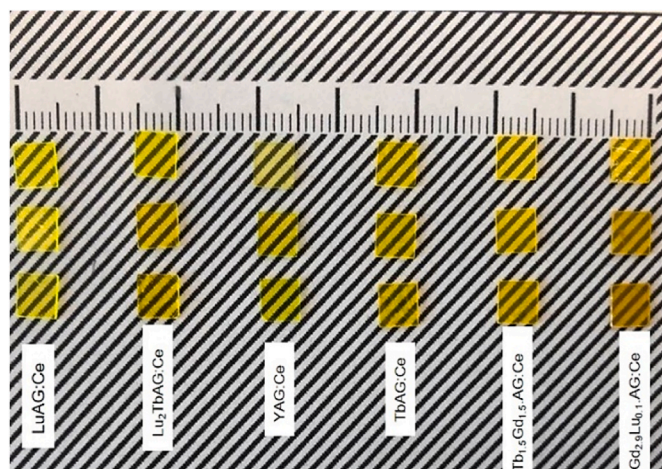


Fig. 1. Photograph of $\{\text{Lu}, \text{Y}, \text{Tb}, \text{Gd}\}_3\text{Al}_5\text{O}_{12}:\text{Ce}$ SCFs with different thicknesses grown by the LPE method onto YAG substrates.

$$R_1 = \frac{P_{\text{fluxPbO}}}{P_{\text{fluxB}_2\text{O}_3}}; R_2 = \frac{\sum P_{\text{garnet}}}{\sum P_{\text{garnet}} + \sum P_{\text{flux}}}; R_3 = \frac{\sum P_{\text{garnet}(\text{dod})}}{\sum P_{\text{garnet}(\text{oct}+\text{tet})}}; R_4 = \frac{\sum P_{\text{dopant}}}{\sum P_{\text{garnet}}} \quad (1a)$$

where P is the mole weights of the garnet and activator host components, which are located in the dodecahedral (dod), octahedral (oct), and tetrahedral (tet) positions in the garnet lattice, as well as the PbO and B_2O_3 flux components.

The solubility of the oxides and the kinetic properties of the solution are both determined mainly by the coefficient $R_1 = 11-12$. The value $R_2 = 0.02-0.035$ identifies the garnet phase as the primary phase during the film crystallization. The choice of molar ratios R_3 and R_4 is directly related to optimizing the structural quality of the SCFs. The optimal values of the coefficients R_3 and R_4 are determined experimentally for SCFs with selected compositions [13].

However, in the case of SCF growth of mixed garnet compounds, the content of different cations in the melt solution can be significantly different in comparison with the actual content of these ions in films. Such difference is caused by different factors such as the various sizes of film cations with respect to cations of substrate lattice, the dimension of the garnet octants (dod., oct. or tet.) for cation localization, the

difference in the film/substrate lattice constant and temperature of film growth. For this reason, the segregation coefficient values of various cations can be taken into account for predicting the demanding SCF content or for estimating the growth content of films grown with nominal garnet content in the melt solution. Namely, the dependence of the segregation coefficient of Lu, Tb and Gd cations and Ce³⁺ activator on the size of these ions in the case of growth A_{1.5}B_{1.5}Al₅O₁₂:Ce (A, B=Lu, Tb, Gd) SCFs onto YAG substrates are presented in Table 1.

It is important to mention also here that molar concentrations of Ce dopant are significantly different in comparison with the real concentration of the activator in the films after the growth process. Namely, the real content of Ce activators in the film (Table 1) is much lower in comparison with the content in the melt solution due to the significantly large size of Ce³⁺ ions with respect to Lu³⁺, Gd³⁺, and Tb³⁺ cations and low temperature of film crystallization (~1000°C) using LPE growth method.

During the LPE growth process the substrate, horizontally attached to a platinum holder, was rotating at 60–80 rpm in the forming melt with growth temperature T_g in the 950–1025 °C range. Under the described conditions, the growth rate was in the f_s = 0.35–1.6 μm/min range. The thickness of the films was determined by weighing them on high-precision scales. To do this, the substrate was weighed before and after the growth cycle of the single crystal. The thickness of SCFs was determined using the formula:

$$h_f = m - m_s / 2Sp \quad (1b)$$

where *m* is the mass of the substrate with the grown single crystalline film in (g), *m_s* sub is the mass of the substrate in (g), *S* is the area of the substrate in (cm²), and *ρ* is the density of the film in (g/cm³) (*ρ* = 4.55 g/cm³ for YAG; 6.67 g/cm³ for LuAG; *ρ* = 6.24 g/cm³ for TbAG).

The actual composition of SCF samples under study (Table 1) was determined using a JEOL JSM-820 electronic microscope, equipped with an EDX microanalyzer with IXRF 500 and LN2 Eumex detectors. From the microanalysis of the content of the SCF samples, we have also found that the segregation coefficient of different cations and Ce³⁺ cations in A_{1.5}B_{1.5}Al₅O₁₂:Ce (A, B=Lu, Tb, Gd) SCFs grown from PbO based flux onto YAG substrates (Table 2).

The XRD measurements using DRON 4 spectrometer (CuK_α X-ray source) were carried out in the 2θ range from 91° to 95° with a step of 0.02° for the determination of the structural quality and misfit values between SCF and YAG:Ce substrate.

Optical absorption spectra of investigated samples were recorded in the 200–1100 nm range using a Jasco 760 UV–Vis spectrometer. The PL emission and excitation (PLE) spectra were recorded with an Edinburgh Instruments FS5 Spectrofluorometer, equipped with a 150 W Xenon lamp as the excitation source. An integration sphere AvaSphere-50-IRRAD coupled with fiber-optic spectrophotometer AvaSpec-uls2048-

Table 2

The segregation coefficients of Lu, Tb and Gd cations and Ce activator in the case of LPE growth A_{1.5}B_{1.5}Al₅O₁₂:Ce (A, B=Lu, Tb, Gd) SCFs onto YAG substrates.

Nominal composition A _{1.5} B _{1.5} Al ₅ O ₁₂	Size of cations/activator in the 8-fold coordination	Segregation coefficient of A ions	Segregation coefficient of B ions	Segregation coefficient of Ce ³⁺ ions
Lu _{1.5} Gd _{1.5} Al ₅ O ₁₂ :Ce	Lu = 0.977 Å Gd = 1.053 Å Ce = 1.143 Å	1.09–1.05 (Lu)	0.91–0.95 (Gd)	0.013–0.016
Lu _{1.5} Tb _{1.5} Al ₅ O ₁₂ :Ce	Lu = 0.977 Å Tb = 1.04 Å Ce = 1.143 Å	0.95–0.85 (Lu)	1.05–1.15 (Tb)	0.009–0.01
Tb _{1.5} Gd _{1.5} Al ₅ O ₁₂ :Ce	Tb = 1.04 Å Gd = 1.053 Å Ce = 1.143 Å	1.18–1.16 (Tb)	0.91–0.94 (Gd)	0.015–0.018

ltec and blue LED 460 nm (30 mA, 2.9V) was used to determine the chromaticity parameters of the samples. The color coordinates, correlated color temperature (CCT), color rendering index (CRI), and luminous efficacy (LE) were calculated using Avantes software. For all measurements, samples with the smallest film thickness from each group of materials were used. Photoconversion results are shown for all samples.

3. Results and discussion

3.1. Structural properties of SCFs

The X-ray phase analysis has confirmed that all the synthesized compounds are single-phase samples containing only the garnet phases and no XRD reflections corresponding to any impurity have been detected. In particular, XRD patterns of {R}₃Al₅O₁₂:Ce; R=Lu, Y, Tb, Gd garnets are shown in Fig. 2a. The dependence of the lattice constant and misfit values on the ionic radius of cations in dodecahedral positions is shown in Fig. 2b. It can be seen that there is an increase of the unit cell parameter with the ionic radius of the cations residing in dodecahedral {Lu³⁺, Y³⁺, Tb³⁺, Gd³⁺} sites, which determines the peak positions of XRD reflections for these garnets.

The lattice mismatch between the substrate and the film was estimated using the formula $m = (a_{\text{film}} - a_{\text{sub}}) / a_{\text{sub}} \times 100$. It is noticeable that the dependencies are linear and consistent with Vegard's law [20]. Small deviations in data are associated with a small variation in the cerium concentration in the samples. The obtained structural data for R₃Al₅O₁₂:Ce; R=Lu, Y, Tb, Gd are systematized in Table 3.

3.2. Optical, luminescence and photoconversion characteristics

The RT absorption spectra of epitaxial structures under study in the 200–550 nm range are shown in Fig. 3. Generally, the absorption bands of Ce³⁺ ions in the studied garnets, detected in the 330–345 nm and 450–465 nm ranges, corresponds to the 4f–5d₂ and 4f–5d₁ transitions, respectively [21]. With increasing of the cation radius in the dodecahedral position of garnet matrix the crystal field strength (CFS) is increasing which consequently shifts the 4f→5d₂ and 4f→5d₁ absorption bands to higher and lower energies, respectively (Fig. 3a). Therefore, the difference between the maxima of E₂ and E₁ bands of Ce³⁺ ions ΔE_{Abs} = E₂ – E₁ is proportional to the values of CFS.

All SCF samples except YAG:Ce and LuAG:Ce SCFs, contain terbium and/or gadolinium ions in the matrix, the absorption lines of which appear in the absorption spectra. Namely, bands centered around ~224 and ~270 nm belong to the low spin-allowed (LS) 4f→5d₂ and 4f→5d₁ absorption transitions of Tb³⁺ ions. The last band is strongly overlapped with bands peaked at 275 nm corresponding to 4f→4f Gd³⁺ transitions. The weak line centered at 373 nm is ascribed to the ⁷F₆→⁵G₆

range in SCF samples is commonly associated with lead flux related dopants, namely by the ¹S₀→³P₁ transitions of Pb²⁺ ions. Such peculiarity is typical for SCF phosphors grown from the PbO-based flux when the Pb²⁺ ions alloyed into the SCF material during the film growth process in a concentration usually below 100 ppm [23].

Cathodoluminescence measurements can provide information about the material content and luminescent properties of Ce³⁺ ions in the different garnet hosts, aiding in the understanding of how they impact the film's overall optical behavior. The normalized RT CL spectra of {Lu, Y, Tb, Gd}₃Al₅O₁₂:Ce SCFs are shown in Fig. 3b. Presented spectra show the dominant doublet emission bands, peaked at 538–598 nm, related to the allowed 5 d¹→ 4f (²F_{5/2;7/2}) transitions of Ce³⁺ ion in garnet hosts. CL spectra of all LPE grown SCF samples demonstrate the absence of the Ce³⁺ luminescence in other phases as well as the luminescence of the defect-related centers (antisite defects and F⁺ centers). This is particularly valuable for devices or applications where maintaining the material's integrity is essential. This phenomenon arises from the extremely low temperature range of 950–1025 °C for SCF crystallization [24]. LPE

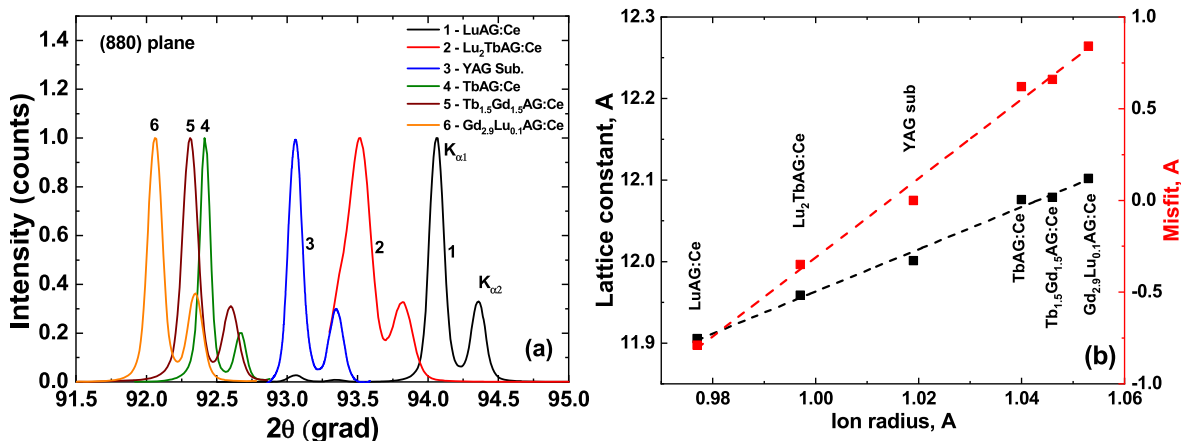


Fig. 2. (a) -XRD pattern of 880 plane of $\{R\}_3\text{Al}_5\text{O}_{12}:\text{Ce}$ ($R=\text{Lu}, \text{Y}, \text{Tb}, \text{Gd}$) SCFs grown on (110) oriented YAG substrate. (b) - dependence of lattice constant on the ionic radius of corresponding garnet forming cations in dodecahedral positions.

Table 3

The values of lattice constant and misfit of garnet SCFs under study with the corresponding ionic radius of R^{3+} cations in the dodecahedral position of $R_3\text{Al}_5\text{O}_{12}:\text{Ce}$ ($R=\text{Lu}, \text{Y}, \text{Tb}, \text{Gd}$) garnets. For mixed garnets, the table shows the average value of the ionic radius in dodecahedral positions (*).

Composition	Ionic radius CN = 8, Å	Lattice constant, Å	Misfit, %
LuAG:Ce	0.977	11.9054	-0.79
Lu ₂ TbAG:Ce	0.997*	11.9588	-0.35
YAG substrate	1.019	12.001	0
TbAG:Ce	1.04	12.076	+0.62
Tb _{1.5} Gd _{1.5} AG:Ce	1.046*	12.0788	+0.66
Gd _{2.9} Lu _{0.1} AG:Ce	1.053	12.102	+0.84

processes allow also selected alloying of film-formated cations into different positions of the garnet host following their ionic radii. That also strongly prevents the formation of antisite defects. LPE is also characterized by the well-controlled cooling process, which can strongly reduce the formation and propagation of macro defects in SCF samples. Slow cooling rates can help in relieving stresses and reducing thermal gradients that might contribute to defect formation [25].

Fig. 4 shows the PL excitation spectra of the Ce^{3+} doped $\{\text{Lu}, \text{Y}, \text{Tb}, \text{Gd}\}_3\text{Al}_5\text{O}_{12}:\text{Ce}$ SCFs set recorded at RT. The excitation spectra of Ce^{3+} emission (540–600 nm) maxima dependent on composition) consist of

two sets of broad bands, which correspond to the absorption spectra belonging to Ce^{3+} and Tb^{3+} ions presented in Fig. 3a. It should be noted that terbium bands are present in all samples, regardless of composition, since Tb^{3+} ions are a trace impurity. The absorption band peaked at 262 nm corresponding to the absorption of Pb^{2+} flux-related impurity in SCFs under study and is caused by the $^1\text{S}_0 \rightarrow ^3\text{P}_1$ transitions of these ions [26].

The bands centered at ~ 239 and ~ 290 nm belong to the low spin-allowed (LS) $4f \rightarrow 5d_2$ and $4f \rightarrow 5d_1$ absorption transitions of Tb^{3+} ions, respectively [27,28]. The weak sharp bands peaked in the 371–378 nm range are ascribed to the $^7\text{F}_6 \rightarrow ^5\text{G}_6$ absorption transitions of Tb^{3+} cations [29]. Also in the $\text{Tb}_{1.5}\text{Gd}_{1.5}\text{Al}_5\text{O}_{12}:\text{Ce}$ and $\text{Gd}_{2.9}\text{Lu}_{0.1}\text{Al}_5\text{O}_{12}:\text{Ce}$ samples the bands peaked at 275 nm and 317 nm are attributed to the $^8\text{S}_{7/2} \rightarrow ^6\text{I}_{3/2-7/2}$ and $^6\text{P}_{7/2} \rightarrow ^8\text{S}_{7/2}$ absorption transitions of the Gd^{3+} cations, respectively. The presence of Tb^{3+} -related bands in the excitation spectrum of the Ce^{3+} luminescence indicates the presence of efficient $\text{Tb}^{3+} \rightarrow \text{Ce}^{3+}$ energy transfer (ET) [30,31].

Table 4 presents the transition energies of the absorption bands of Ce^{3+} in the studied samples extracted from Fig. 4a. The splitting between the $5d_2$ and $5d_1$ states, expressed as the difference in the position of the E2 and E1 excitation bands, is given for all specimens. The observed change in the splitting energy suggests that the crystal field strength in the dodecahedral site, where Ce^{3+} ions are localized, exhibits

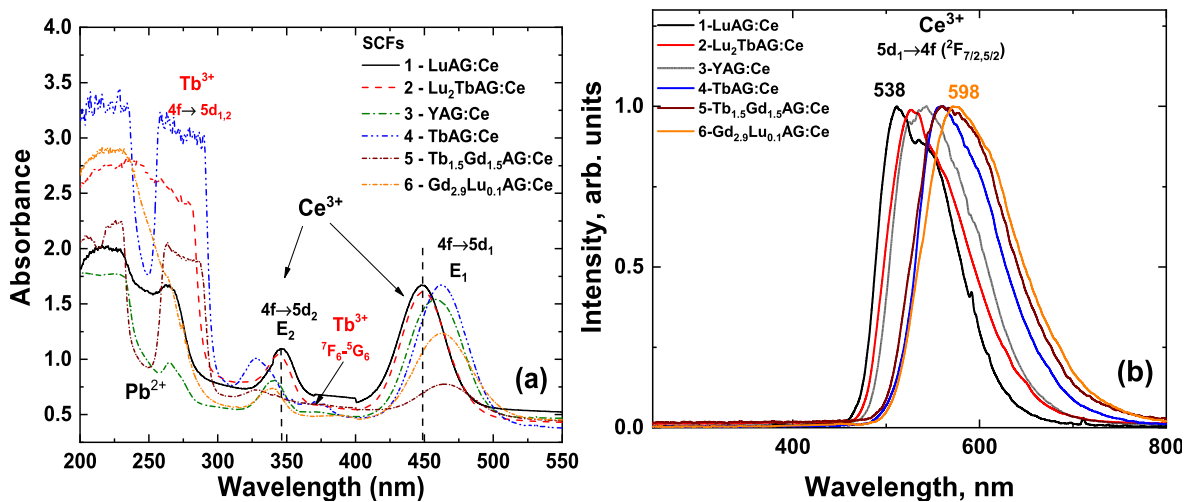


Fig. 3. RT absorption (a) and CL (b) spectra of $\{\text{Lu}, \text{Y}, \text{Tb}, \text{Gd}\}_3\text{Al}_5\text{O}_{12}:\text{Ce}$ SCFs converters. absorption transitions of Tb^{3+} cations [22]. Minor absorption bands are related to $4f \rightarrow 4f$ Gd^{3+} transitions, peaked in the 313–317 nm range, and overlapped with bands related to the high spin-allowed (HS) $4f \rightarrow 5d_1$ transitions of Tb^{3+} ions. Furthermore, the UV absorption band at 262–265 nm.

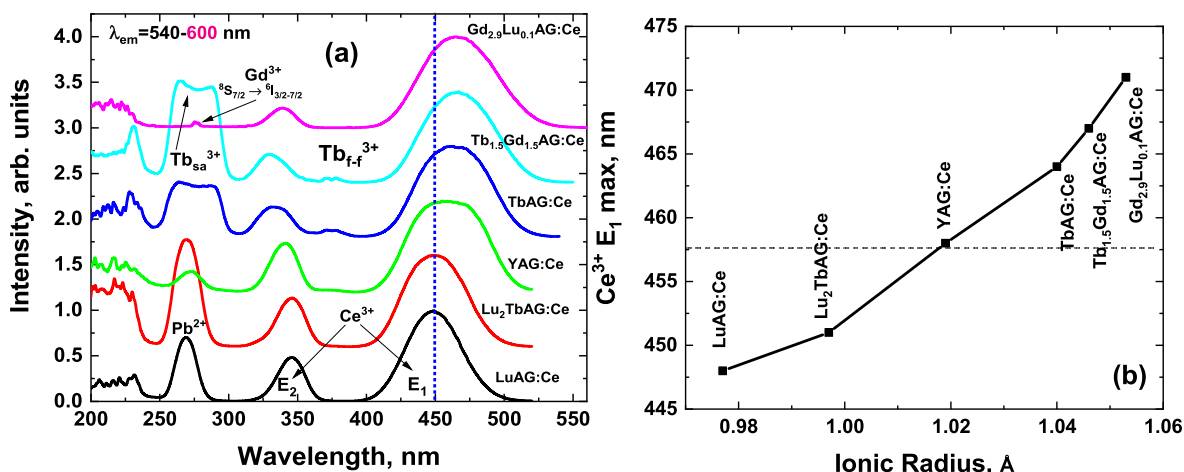


Fig. 4. (a) - RT excitation spectra of the Ce³⁺ emission at 540–600 nm (emission maxima) in (b) - dependence of Ce³⁺ E₁ excitation maxima on the ionic radius of corresponding garnet forming cations in dodecahedral positions.

Table 4

The Ce³⁺ absorption transition energies in {Lu, Y, Tb, Gd}₃Al₅O₁₂:Ce SCFs at RT.

Composition	Absorption bands		
	E1 (4f→5d ¹), (eV)	E2 (4f→5d ²), (eV)	Splitting (eV)
Lu ₃ Al ₅ O ₁₂ :Ce	2.77 (448 nm)	3.56 (348 nm)	0.79
Lu ₂ TbAl ₅ O ₁₂ :Ce	2.75 (451 nm)	3.59 (345 nm)	0.84
Y ₃ Al ₅ O ₁₂ :Ce	2.71 (458 nm)	3.63 (341 nm)	0.93
Tb ₃ Al ₅ O ₁₂ :Ce	2.67 (464 nm)	3.72 (333 nm)	1.05
Tb _{1.5} Gd _{1.5} Al ₅ O ₁₂ :Ce	2.65 (467 nm)	3.76 (330 nm)	1.11
Gd _{2.9} Lu _{0.1} Al ₅ O ₁₂ :Ce	2.63 (471 nm)	3.67 (338 nm)	1.04

an upward trend as the ion radius increases in the dodecahedral site of the garnet host. Fig. 4b shows the dependence of the 4f (²F_{5/2}) → 5d₁ (E_{2g}) absorption transition maximum on the ion radius in dodecahedral positions. This intense band is suitable for blue InGaN LED excitation because the emission wavelength of blue LED chips is in the 450–480 nm range. The blue dashed line in Fig. 4 indicates the emission maxima of commercial blue LED (450 nm), in combination with which, the photoconversion properties of SCFs were investigated in this work.

The PL emission spectra of (Lu, Y, Tb, Gd)₃Al₅O₁₂:Ce SCFs excited at 460 nm (Fig. 5a) present broad yellow emission, related to the electronic transitions from the first excited state to the two ground state levels (²F_{5/2}, ²F_{7/2}) of Ce³⁺ ions. In comparison with LuAG:Ce SCF, the Ce³⁺ emission maxima in Gd_{2.9}Lu_{0.1}Al₅O₁₂:Ce SCFs is significantly red shifted

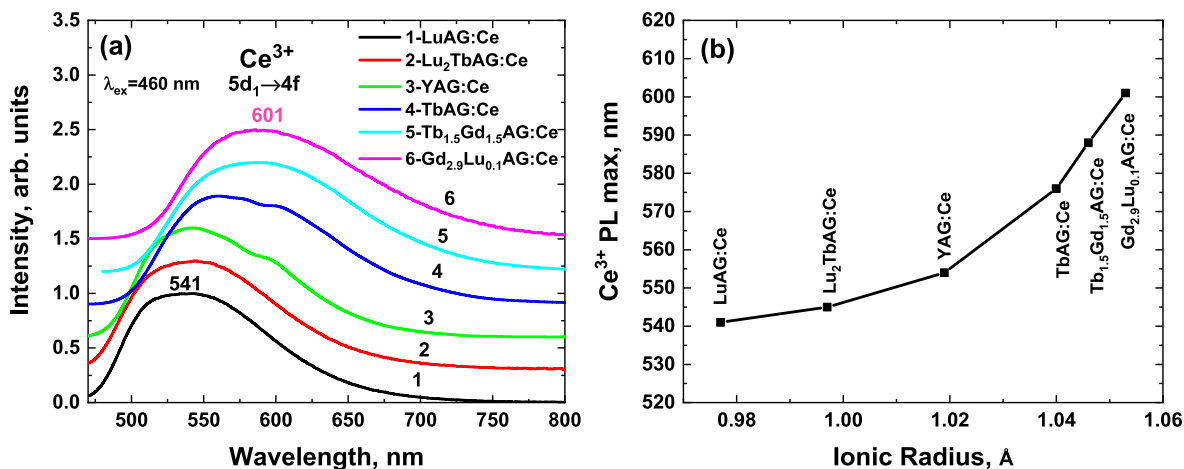


Fig. 5. (a) - RT PL emission spectra of the Ce³⁺ in (Lu, Y, Tb, Gd)₃Al₅O₁₂:Ce SCFs excited at 460 nm (maxima of commercial blue LED), (b) - dependence of Ce³⁺ emission maxima on the ionic radius of corresponding garnet forming cations in dodecahedral positions.

from 541 to 601 nm. This phenomenon is illustrated by the dependence of Ce³⁺ emission maxima on the ionic radius of corresponding garnet cations in dodecahedral positions, presented in Fig. 5b. The trend of this dependence shows the potential possibility of controlling the Ce³⁺ emission spectrum in the case of the application of the films under study as photoconverters of WLEDs.

3.3. Photoconversion properties

Prototypes of pc-WLEDs were manufactured to assess device performance and determine the dependence of colorimetric parameters on SCF converter's thickness. The spectra corresponding to WLEDs, which were created by mounting SCF converters with different thicknesses onto InGaN blue 450 nm emitting chips (operated with a forward-bias voltage of 2.9 V and a current drive of 20 mA), are presented in Fig. 6. These spectra have been normalized on the maximum of the yellow emission component.

In this lighting system, two strong spectral bands attributed to the excitation of blue LED and broad emission in 500–800 nm range correspond to the emission of the converter, respectively. Due to the increase in film thickness, the blue light originating from the blue chip decreases continuously, and the yellow light originating from YAG:Ce SCF increases. This is well accordance with the absorbance spectra shown in Fig. 3a. Depending on the composition of the SCFs, the shape and intensity of the blue component changes due to the shift of the Ce³⁺

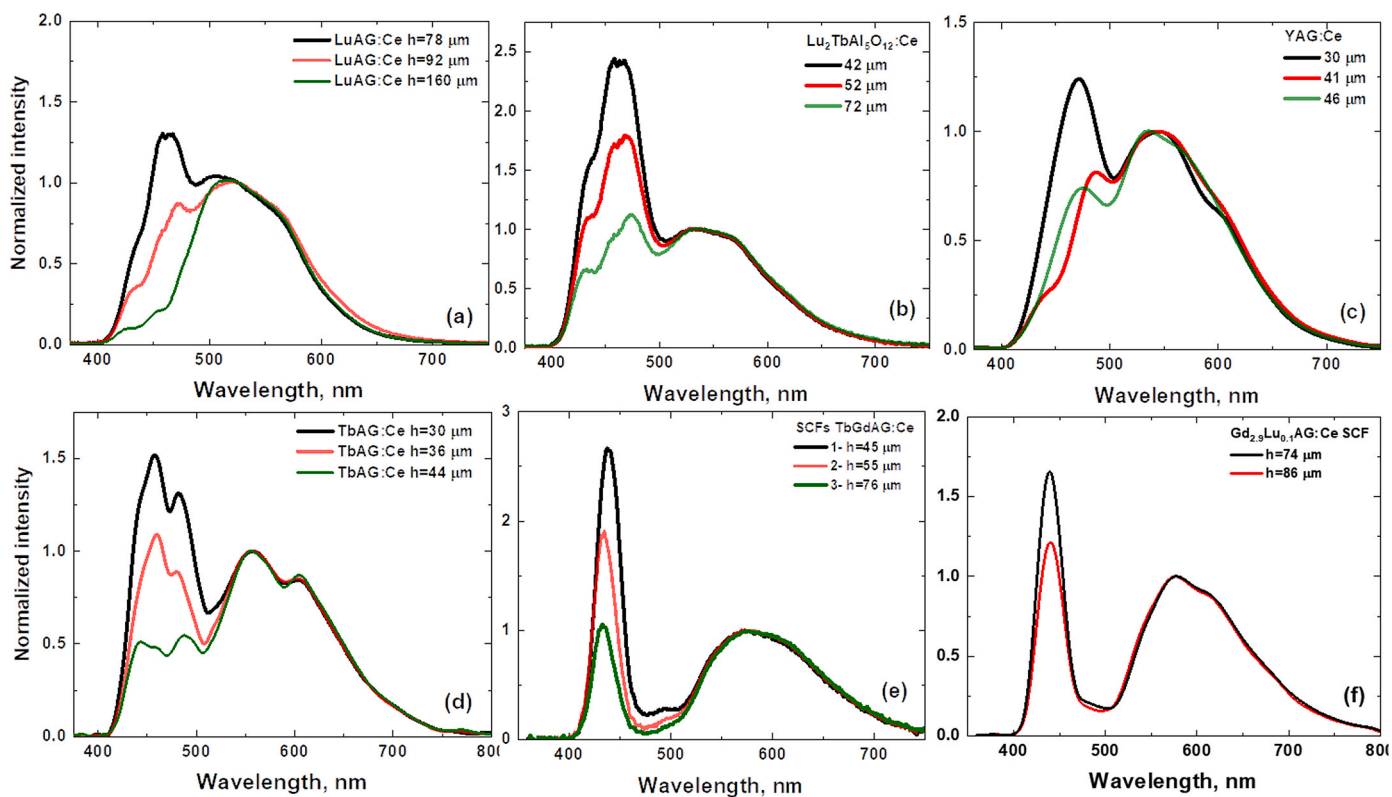


Fig. 6. The spectral performance of SCF converters under blue LED excitation; (a) - LuAG:Ce, (b) - Lu₂TbAG:Ce, (c) - YAG:Ce, (d) - TbAG:Ce, (e) - Tb_{1.5}Gd_{1.5}AG:Ce, (f) - Gd_{2.9}Lu_{0.1}AG:Ce.

E₁ absorption maximum (Fig. 5b). Due to the changing emission intensities of blue chip and Ce³⁺ ions, the photometric and chromatic parameters of the WLED devices were subsequently different.

The CCT and the color rendering index (CRI) decrease with increasing film thickness, due to higher absorption of blue light and stronger emission of yellow light. Fig. 7 shows the change of WLED device's colors based on WLED emission spectra (Fig. 6). Based on Fig. 6, it can be seen that the shift of color coordinates from the green to the red region during the transition from LuAG:Ce (Fig. 6a) to Gd_{2.9}Lu_{0.1}AG:Ce (f), which corresponds to the red shift in the PL spectra (Fig.

5). However, it is also seen that in these two boundary compositions from the studied series of garnets, a higher film thickness is necessary to obtain color coordinates in the central part of the diagram. This is explained by the greater intensity of the blue component, due to the weak overlap between the absorption lines of the converter and the emission line of the blue LED.

Table 5 lists the CIE coordinates, correlated color temperature (CCT), and color rendering index (CRI) values.

4. Conclusions

The investigation of structural, luminescence and photoconversion properties of the single crystalline films (SCF) of Ce³⁺ doped R₃Al₅O₁₂:Ce (R=Lu, Y, Tb, Gd) mixed garnet was performed in this work. The SCFs were grown using the liquid phase epitaxy (LPE) method onto YAG crystal substrates from melt-solutions based on the PbO–B₂O₃ based flux. The content analysis of the obtained SCF samples, grown from the melt-solution with nominal molar composition Lu₃Al₅O₁₂, Lu₂TbAl₅O₁₂, Y₃Al₅O₁₂, Tb_{1.5}Gd_{1.5}Al₅O₁₂ and Gd_{2.9}Lu_{0.1}Al₅O₁₂, and Ce activator content in the 8–12 mol % range confirm the crystallization of Lu₃Al₅O₁₂:Ce (0.075 at.%), Lu_{1.85}Tb_{1.15}Al₅O₁₂:Ce (1 at.%), Y₃Al₅O₁₂:Ce (1 at.%), Tb₃Al₅O₁₂:Ce (1 at.%), Tb_{1.62}Gd_{1.38}Al₅O₁₂:Ce (1.5 at.%) and Gd_{2.84}Lu_{0.16}Al₅O₁₂:Ce (1.5 at.%) SCF samples. The XRD analyses of

these SCFs confirm their high structural quality, despite the large SCF-substrate lattice misfit ranging in $-0.79\% - +0.84\%$ range. The segregation coefficients of Lu, Gd and Tb cations and Ce³⁺ ions at the crystallization SCF of A_{1.5}B_{1.5}Al₅O₁₂:Ce (A, B=Lu, Gd; Tb) mixed garnets onto Y₃Al₅O₁₂ substrates were found as well.

The optical properties of SCFs samples were characterized in this work using absorption, cathodo- and photoluminescence spectra. The photoconversion properties of all SCFs with different thicknesses in the 22–162 μm range (color coordinates, correlated color temperature (CCT) and color rendering index (CRI)) were performed as well under excitation by 455 nm commercial blue LED.

We have found that using LPE growth method, it is possible to obtain a series of R₃Al₅O₁₂:Ce (R=Lu, Y, Tb, Gd) SCF phosphor converters onto one type of substrate (YAG) with varying photoconversion parameters. In general, the application of such SCF converters covers all colors close to the theoretically white point on the color diagram. Furthermore, the dependence of photoconversion properties on the film thicknesses was studied to construct the prototypes of efficient warm WLEDs. The systematic variation in the film thickness in the 22–162 μm range enables tuning the white light tones from cold white/daylight white (CCT >6000 K) to neutral white (6000 K > CCT >3300 K). We have found also that the CCT values decrease and the CRI increase with increasing of R₃Al₅O₁₂:Ce (R=Lu, Y, Tb, Gd) SCF film thickness due to higher absorption of blue light and stronger emission of yellow light. Meanwhile, the CRI values were higher and CCT values were lower for all TbAG:Ce based SCFs compared with other film converters under study.

These experiments provide also valuable insights into the optimal combinations of composition and thickness of single crystalline converters for efficient WLED with extremely high stability and durability of parameters.

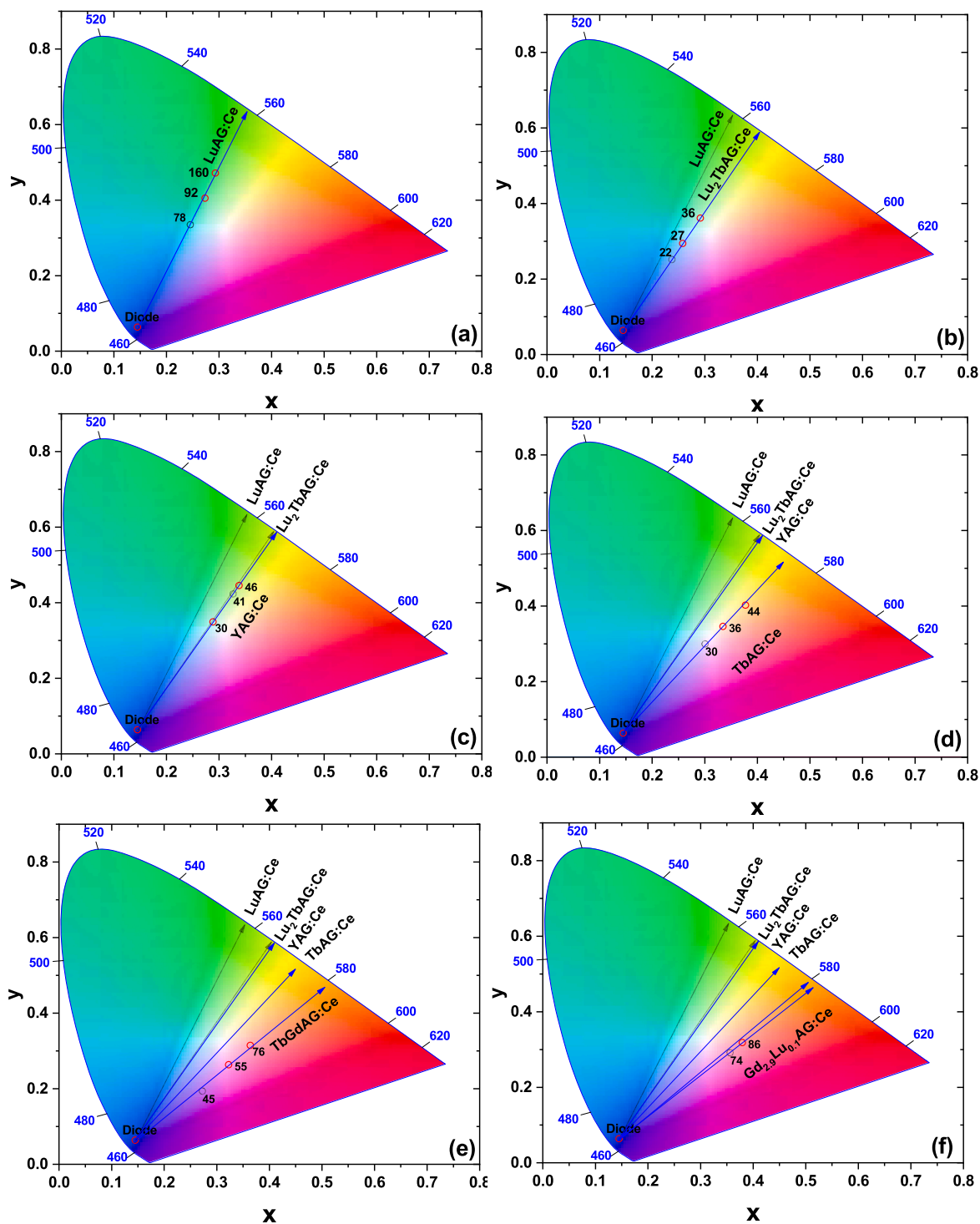


Fig. 7. The CIE diagrams of SCF converters under blue LED excitation; (a) -LuAG:Ce, (b)- Lu₂TbAG:Ce, (c) - YAG:Ce, (d) - TbAG:Ce, (e) - Tb_{1.5}Gd_{1.5}AG:Ce, (f) - Gd_{2.9}Lu_{0.1}AG:Ce.

Funding

The work was performed in the frame of Polish NCN 2022/45/B/ST8/01757 projects and partly in the frame of NCN 2018/31/B/ST8/03390 projects.

Author contributions

Anton Markovskiy performed photoconversion measurements of

SCFs, analyzed experimental materials, and wrote the manuscript, Vitalii Gorbenko performed the SCFs growth by the LPE method; Tetiana Zorenko performed the absorption, photoluminescence, Alexander Fedorov performed the XRD measurements, Yuriy Zorenko performed the conception of work, analyzed results in the whole of the paper and edited the final version of the manuscript.

Table 5
Photoconversion properties of (Lu,Y,Tb,Gd)₃Al₅O₁₂:Ce SCF converters in combination with blue LED.

h, μm	x	y	CCT, K	CRI
LuAG:Ce				
78	0.301	0.3063	–	–
92	0.3351	0.3454	11,630	59
162	0.3778	0.4017	7569	57
Lu₂Tb₁AG:Ce				
22	0.238	0.250	–	–
27	0.258	0.293	11,980	–
36	0.292	0.360	7281	72
YAG:Ce				
30	0.288	0.355	7481	74
41	0.327	0.422	5665	66
46	0.338	0.445	5365	66
h, μm	x	y	CCT, K	CRI
TbAG:Ce				
30	0.301	0.306	7516	88
36	0.335	0.345	5387	86
44	0.377	0.401	4226	78
TbGdAG:Ce				
45	0.272	0.193	–	–
55	0.323	0.263	6361	78
76	0.364	0.314	3971	73
Gd_{2.9}Lu_{0.1}AG:Ce				
74	0.356	0.290	4029	77
86	0.374	0.323	3686	74

Declaration of competing interest

We wish to confirm that there are no known conflicts of interest associated with this publication and there has been no significant financial support for this work that could have influenced its outcome.

We confirm that the manuscript has been read and approved by all named authors and that there are no other persons who satisfied the criteria for authorship but are not listed. We further confirm that the order of authors listed in the manuscript has been approved by all of us.

We confirm that we have given due consideration to the protection of intellectual property associated with this work and that there are no impediments to publication, including the timing of publication, with respect to intellectual property. In so doing we confirm that we have followed the regulations of our institutions concerning intellectual property.

We understand that the Corresponding Author is the contact for the Editorial process (including Editorial Manager and direct communications with the office). He/she is responsible for communicating with the other authors about progress, submissions of revisions and final approval of proofs. We confirm that we have provided a current, correct email address which is accessible by the Corresponding Author and which has been configured to accept email from a.mark@ukw.edu.pl; zorenko@ukw.edu.pl.

Data availability

No data was used for the research described in the article.

References

- K. Kamada, T. Endo, K. Tsutsumi, T. Yanagida, Y. Fujimoto, A. Fukabori, A. Yoshikawa, J. Pejchal, M. Nikl, Composition engineering in cerium-doped (Lu, Gd)₃(Ga,Al)₅O₁₂ single-crystal scintillators, *Cryst. Growth Des.* 11 (2011) 4484–4490, <https://doi.org/10.1021/cg200694a>.
- M. Fasoli, A. Vedda, M. Nikl, C. Jiang, B.P. Uberuaga, D.A. Andersson, K. J. McClellan, C.R. Stanek, Band-gap engineering for removing shallow traps in rare-earth Lu₃Al₅O₁₂ garnet scintillators using Ga³⁺ doping, *Phys. Rev. B Condens. Matter* 84 (2011), <https://doi.org/10.1103/physrevb.84.081102>.
- G. Li, Y. Tian, Y. Zhao, J. Lin, Recent progress in luminescence tuning of Ce³⁺ and Eu²⁺-activated phosphors for pc-WLEDs, *Chem. Soc. Rev.* 44 (2015) 8688–8713, <https://doi.org/10.1039/c4cs00446a>.
- J. Chen, Y. Tang, X. Yi, Y. Tian, G. Ao, D. Hao, Y. Lin, S. Zhou, Fabrication of (Tb, Gd)₃Al₅O₁₂:Ce³⁺ phosphor ceramics for warm white light-emitting diodes application, *Opt. Mater. Express* 9 (2019) 3333, <https://doi.org/10.1364/ome.9.003333>.
- S. Arjoca, D. Inomata, Y. Matsushita, K. Shimamura, Growth and optical properties of (Y_{1-x}Gd_x)₃Al₅O₁₂:Ce single crystal phosphors for high-brightness neutral white LEDs and LDs, *Cryst. Eng. Comm.* 18 (2016) 4799–4806, <https://doi.org/10.1039/C6CE00500D>.
- Z.-T. Li, Y.-J. Chen, J.-S. Li, S.-M. Liang, Y. Tang, Toward one-hundred-watt-level applications of quantum dot converters in high-power light-emitting diode system using water-cooling remote structure, *Appl. Therm. Eng.* 179 (2020), 115666, <https://doi.org/10.1016/j.applthermaleng.2020.115666>.
- T.W. Kang, K.W. Park, J.H. Ryu, S.G. Lim, Y.M. Yu, J.S. Kim, Strong thermal stability of Lu₃Al₅O₁₂:Ce³⁺ single crystal phosphor for laser lighting, *J. Lumin.* 191 (2017) 35–39, <https://doi.org/10.1016/j.jlumin.2017.01.032>.
- K. Bartosiewicz, V. Babin, J.A. Mares, J.A. Mares, Y. Zorenko, A. Iskalyeva, V. Gorbenko, Z. Brykhar, M. Nikl, Luminescence and energy transfer processes in Ce³⁺ activated (Gd,Tb)₃Al₅O₁₂ single crystalline films, *J. Lumin.* 188 (2017) 60–66, <https://doi.org/10.1016/j.jlumin.2017.04.010>.
- E.G. Villora, S. Arjoca, D. Inomata, K. Shimamura, Single-crystal phosphors for high-brightness white LEDs/LDs, in: H. Jeon, L.-W. Tu, M.R. Krames, M. Strassburg (Eds.), *Light-Emitting Diodes: Materials, Devices, and Applications for Solid State Lighting XX*, SPIE, 2016.
- P. Capper, M.D. Mauk (Eds.), *Liquid Phase Epitaxy of Electronic, Optical and Optoelectronic Materials: Copper/Liquid Phase Epitaxy of Electronic, Optical and Optoelectronic Materials, first ed.*, Wiley-Blackwell, Hoboken, NJ, 2007.
- Y. Zorenko, V. Gorbenko, Growth peculiarities of the (Y, Tb, Eu–Y) single crystalline film phosphors by liquid phase epitaxy, *Radiat. Meas.* 42 (2007) 907–910, <https://doi.org/10.1016/j.radmeas.2007.02.049>.
- Y. Zorenko, V. Gorbenko, J. Vasylyuk, A. Zeleny, A. Fedorov, R. Kucerkova, J. A. Mares, M. Nikl, P. Bilski, A. Twardak, Growth and luminescent properties of scintillators based on the single crystalline films of Lu_{3-x}Gd_xAl₅O₁₂:Ce garnet, *Mater. Res. Bull.* 64 (2015) 355–363, <https://doi.org/10.1016/j.materresbull.2015.01.020>.
- S. Witkiewicz-Lukaszek, V. Gorbenko, T. Zorenko, Y. Syrotych, J.A. Mares, M. Nikl, O. Sidletskiy, P. Bilski, A. Yoshikawa, Y. Zorenko, Composite detectors based on single-crystalline films and single crystals of garnet compounds, *Materials* 15 (2022) 1249, <https://doi.org/10.3390/ma15031249>.
- V.P. Dotsenko, I.V. Berezovskaya, A.S. Voloshinovich, B.I. Zadneprovskii, N. P. Efruyshina, Luminescence properties and electronic structure of Ce³⁺-doped gadolinium aluminum garnet, *Mater. Res. Bull.* 64 (2015) 151–155, <https://doi.org/10.1016/j.materresbull.2014.12.056>.
- C.-C. Chiang, M.-S. Tsai, M.-H. Hon, Preparation of cerium-activated GAG phosphor powders, *J. Electrochem. Soc.* 154 (2007) J326, <https://doi.org/10.1149/1.2768900>.
- J.M. Ogieglo, A. Katelnikovas, A. Zych, T. Jüstel, A. Meijerink, C.R. Ronda, Luminescence and luminescence quenching in Gd₃(Ga,Al)₅O₁₂ scintillators doped with Ce³⁺, *J. Phys. Chem. A* 117 (2013) 2479–2484, <https://doi.org/10.1021/jp309572p>.
- G. Liu, B. Wang, J. Li, B. Cao, Y. Lu, Z. Liu, Research progress of gadolinium aluminum garnet based optical materials, *Physica B Condens. Matter* 603 (2021), 412775, <https://doi.org/10.1016/j.physb.2020.412775>.
- D. Kundaliya, M. Raukas, A.M. Scotch, D. Hamby, K. Mishra, M.U.S. Stough, *Wavelength Converter for an LED and LED Containing Same*, 2015, p. 937, https://www.ukw.edu.pl/download/59310/European_Patent_Application.pdf.
- A. Nakatsuka, A. Yoshiasa, T. Yamanaka, Cation distribution and crystal chemistry of Y₃Al_{5-x}Ga_xO₁₂ (0 ≤ x ≤ 5) garnet solid solutions, *Acta Crystallogr. B* 55 (1999) 266–272, <https://doi.org/10.1107/s0108768198012567>.
- P.A. Tanner, L. Fu, L. Ning, B.-M. Cheng, M.G. Brik, Soft synthesis and vacuum ultraviolet spectra of YAG:Ce³⁺ nanocrystals: reassignment of Ce³⁺ energy levels, *J. Phys. Condens. Matter* 19 (2007), 216213, <https://doi.org/10.1088/0953-8984/19/21/216213>.
- A.A. Setlur, J.J. Shiang, C.J. Vess, Transition from long-range to short-range energy transfer through donor migration in garnet hosts, *J. Phys. Chem. C Nanomater. Interfaces* 115 (8) (2011) 3475–3480, <https://doi.org/10.1021/jp110520j>.
- J.M. Robertson, M.J.G. van Hout, J.C. Verplanke, J.C. Brice, Lead incorporation in thin iron garnet films produced by LPE and chemical analysis by the radioactive tracer technique, *Mater. Res. Bull.* 9 (1974) 555–567, [https://doi.org/10.1016/0025-5408\(74\)90125-1](https://doi.org/10.1016/0025-5408(74)90125-1).
- Y. Zorenko, V. Gorbenko, T. Voznyak, M. Batentschuk, A. Osvet, A. Winnacker, Luminescence of Mn²⁺ ions in Tb₃Al₅O₁₂ garnet, *J. Lumin.* 130 (2010) 380–386, <https://doi.org/10.1016/j.jlumin.2009.09.024>.
- C.W. Wilkins, G.P. Gill, The preparation of low defect density LPE garnet films for magnetic bubble device fabrication, *J. Cryst. Growth* 47 (1979) 299–309, [https://doi.org/10.1016/0022-0248\(79\)90255-0](https://doi.org/10.1016/0022-0248(79)90255-0).
- S. Zazubovich, A. Krasnikov, Y. Zorenko, V. Gorbenko, V. Babin, E. Mihokova, M. Nikl, Chapter 6 luminescence of Pb and Bi-related centers in aluminum garnet, perovskite, and orthosilicate single-crystalline films, in: *Nanocomposite, Ceramic and Thin Film Scintillators*, Pan Stanford Publishing, Penthouse Level, Suntec Tower 3, 8, Temasek Boulevard, Singapore, 2017, pp. 227–302, 038988.
- R. Turos-Matysiak, W. Gryk, M. Grinberg, Y.S. Lin, R.S. Liu, *J. Phys. Condens. Matter* 18 (2006), 10531.
- B.D. Joshi, A.G. Page, *J. Lumin.* 6 (1973) 441.
- K. Bartosiewicz, V. Babin, A. Beitelrova, P. Bohacek, K. Jurek, M. Nikl, The temperature dependence studies of rare-earth (Dy³⁺, Sm³⁺, Eu³⁺ and Tb³⁺)

- activated $\text{Gd}_3\text{Ga}_3\text{Al}_2\text{O}_{12}$ garnet single crystals, *J. Lumin.* 189 (2017) 126–139, <https://doi.org/10.1016/j.jlumin.2016.09.053>.
- [30] R. Tuross-Matysiak, W. Gryk, M. Grinberg, Y.S. Lin, R.S. Liu, Tb^{3+} - Ce^{3+} Energy transfer in $\text{Y}_{3-x}\text{Tb}_x\text{Gd}_y\text{Al}_5\text{O}_{12}$, ($x=0.65$, $y=0.575$) doped with Ce^{3+} , *Radiat Measure* 42 (2007) 755–758, <https://doi.org/10.1016/j.radmeas.2007.02.003>.
- [31] M. Zhuravleva, K. Yang, M. Spurrier-Koschan, P. Szupryczynski, A. Yoshikawa, C. L. Melcher, Crystal growth and characterization of LuAG:Ce:Tb scintillator, *J. Cryst. Growth* 312 (2010) 1244–1248, <https://doi.org/10.1016/j.jcrysgr.2009.11.021>.